

# Long-term preservation of cone photoreceptors and visual acuity in rd10 mutant mice exposed to continuous environmental enrichment

Ilaria Barone,<sup>1</sup> Elena Novelli,<sup>2</sup> Enrica Strettoi<sup>1</sup>

<sup>1</sup>CNR Neuroscience Institute, Pisa, Italy; <sup>2</sup>GB Bietti Foundation for Ophthalmology, Rome, Italy

**Purpose:** In human patients and animal models of retinitis pigmentosa (RP), a gradual loss of rod photoreceptors and decline in scotopic vision are the primary manifestations of the disease. Secondary death of cones and gradual, regressive remodeling of the inner retina follow and progress at different speeds according to the underlying genetic defect. In any case, the final outcome is near-blindness without a conclusive cure yet. We recently reported that environmental enrichment (EE), an experimental manipulation based on exposure to enhanced motor, sensory, and social stimulation, when started at birth, exerts clear beneficial effects on a mouse model of RP, by slowing vision loss. The purpose of this study was to investigate in the same mouse the long-term effects of chronic exposure to an EE and assess the outcome of this manipulation on cone survival, inner retinal preservation, and visual behavior.

**Methods:** Two groups of rd10 mutant mice were maintained in an EE or standard (ST) laboratory conditions up to 1 year of age. Then, retinal preservation was assessed with immunocytochemistry, confocal microscopy examination, cone counts, and electron microscopy of the photoreceptor layer, while visual acuity was tested behaviorally with a Prusky water maze.

**Results:** rd10 mice are a model of autosomal recessive RP with a typical rod-cone, center to the periphery pattern of photoreceptor degeneration. They carry a mutation of the rod-specific phosphodiesterase gene and undergo rod death that peaks at around P24, while cone electroretinogram (ERG) is extinct by P60. We previously showed that early exposure to an EE efficiently delays photoreceptor degeneration in these mutants, extending the time window of cone viability and cone-mediated vision well beyond the phase of maximum rod death. Here we find that a maintained EE can delay the degeneration of cones even in the long term. Confocal and electron microscopy examination of the retinas of the rd10 EE and ST mice at 1 year of age showed major degeneration of the photoreceptor layer in both experimental groups, with small clusters of photoreceptors persisting in the peripheral retina. These vestigial cells were positive for L and M opsins and cone arrestin and represented the residual population of cones. In the retinas of the EE mice, cones were more numerous and less remodeled than in the ST counterparts, albeit virtually devoid of outer segments, as confirmed with electron microscopy (EM) observations. Cone counting in retinal whole mounts showed that rd10 EE mice at 1 year had almost three times as many surviving cones ( $34,000 \pm 4,000$ ) as the ST control mice ( $12,700 \pm 1,800$ ), *t* test  $p=0.003$ . Accordingly, the rd10 EE mice at 1 year of age were still capable of performing the visual water task in photopic conditions, showing a residual visual acuity of  $0.138 \pm 0$  cycles/degree. This ability was virtually absent in the rd10 ST age-matched mice ( $0.063 \pm 0.014$ ), *t* test,  $p=0.029$ . No major differences were detected in the morphology of the neurons of the inner retina between the two experimental groups.

**Conclusions:** The approaches used to test the effects of an EE were consistent in showing significantly better preservation of cones and measurable visual acuity in 1-year-old rd10 EE mice. We therefore confirm and extend previous findings that showed an EE is an effective, minimally invasive tool for promoting long-lasting retinal protection in experimental models of RP.

Studies of age-related neuronal changes in the visual system of mice show a consistent decline in visual acuity and contrast sensitivity in time [1]. Lehmann et al. (2012)

demonstrated that reduced visual function in aging is determined not only by a progressive retinal deficiency but also by changes in cortical plasticity [2]. In turn, plasticity is influenced by strictly organic processes that affect the cerebral structure, biochemistry, and physiology during aging as well as by individual life-history events and environmental factors. Environmental enrichment (EE) is an experimental manipulation based upon the exposure of laboratory animals to increased multisensorial, motor, and social stimulation. A wealth of literature shows that an EE represents a general paradigm to burst central nervous system (CNS) plasticity, as

---

Correspondence to: Enrica Strettoi, Istituto di Neuroscienze del CNR, Via Moruzzi 1, 56100 Pisa, Italy; Phone: (39) 050 3153213; FAX: (39) 050 3153212; email: [enrica.strettoi@in.cnr.it](mailto:enrica.strettoi@in.cnr.it)  
 Ilaria Barone is now at Dulbecco Telethon Institute, Dip. Endocrinologia e Metabolismo, Ospedale di Cisanello, Via Paradisa 2, 56124 Pisa, Italy. Elena Novelli is now at Istituto di Neuroscienze del CNR, Via Moruzzi 1, 56100 Pisa, Italy; email: [enrica.strettoi@in.cnr.it](mailto:enrica.strettoi@in.cnr.it)

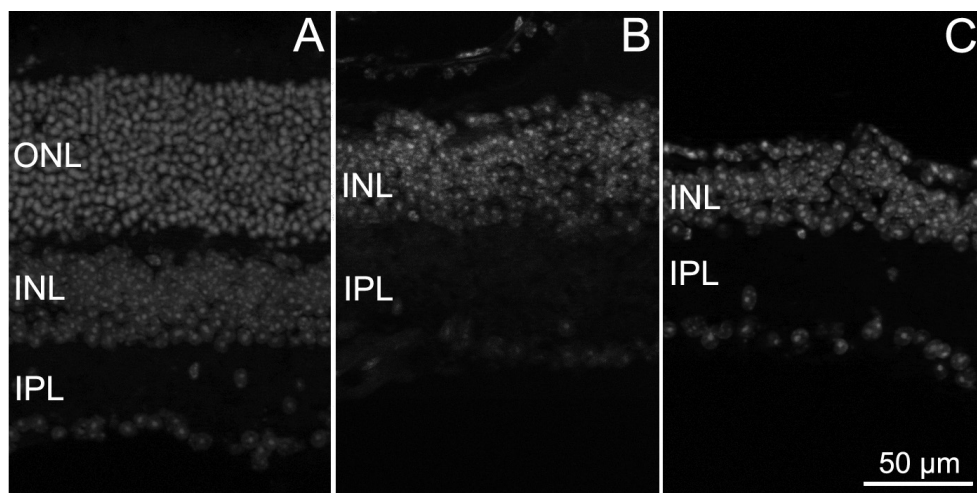


Figure 1. Retinal degeneration in rd10 EE and ST mice. Fluorescence nuclear staining of vertical retinal sections obtained from a WT mouse (A), an rd10 EE mouse (B), and an rd10 ST mouse (C), all aged 1 year. Extensive photoreceptor degeneration with the disappearance of the outer nuclear layer (ONL) is clear in B and C. The sample in C also shows highly irregular outer and inner retinal margins, typical of the extremely thin and fragile retinas of rd10 ST mice of this age. INL = inner nuclear layer; IPL = inner plexiform layer.

well as a useful tool for enhancing neuroprotection in pathological conditions [3-5]. In line with the literature showing the positive effects of an EE in ameliorating the symptoms of amblyopia [6], Alzheimer disease, Rett syndrome, and other CNS disorders in laboratory animals [4], our recent work has shown that an EE preserves the retinal structure and visual function in a mouse model of retinitis pigmentosa (RP). In this well-known family of inherited disorders, typically, a mutation in a retinal-specific gene causes the primary degeneration of rods, followed by the secondary death of cones, to near blindness [7].

Given the complex molecular etiology of RP (in which hundreds of mutations in different genes lead to a similar phenotype) [8], understanding and treating this disease pose a major challenge. Among various therapeutic approaches, those based on neuroprotection, either in the form of vitamin supplementation, antioxidants, administration of trophic factors, or survival molecules, given directly or by gene-therapy approaches, share the goal of further delaying a naturally slow disease, thus prolonging the time window of useful vision [9,10]. Particularly important is preventing the secondary loss of cones by targeting factors that concur with the degeneration of these cells, which represents the main cause of life quality deterioration in human patients with RP. The main aim of the present work was to investigate the long-term effects of an EE as an experimental strategy for slowing cone vision decline in a well-known model of RP, the rd10 mouse, which carries a recessive mutation of the beta subunit of the rod-specific phosphodiesterase gene [11]. In a previous study in which an EE was used for the first time in a paradigm of inherited retinal degeneration,

we demonstrated that in rd10 mice born and maintained in spacious cages and in large social groups with objects specifically devoted to multisensory, cognitive, and motor stimulation, the loss of rod photoreceptors and the secondary death of cones are delayed, and therefore, vision and visual behavior are preserved in time [12]. This initial study spanned the time period of 1–3 months of age. The data reported in the present work were obtained from a group of rd10 mice born and raised in enriched conditions up to 1 year of age. Retinal morphology, ultrastructure, and visual behavior of the mice were compared to those of age-matched rd10 mice kept in standard (ST) laboratory conditions. Although the number of animals that could be examined was understandably small, given the long observational period, the long-term, beneficial effects of an EE on cone viability were clearly demonstrated.

## METHODS

### *Animals:*

**Ethics statement**—All procedures were performed according to the guidelines of the Italian Ministry of Health for care and maintenance of laboratory animals (law 116/92) and in compliance with the European Communities Council Directive n. 86/609/EEC. Animal experimentation at the CNR Neuroscience Institute was approved by the Italian Ministry of Health (authorization # 129/2000-A). The experimental protocol specifically described in this study was authorized by the Italian Ministry of Health (decree #185/2009-B, released on 11/04/2009).

Retinal tissue was obtained from animals deeply anesthetized with intraperitoneal injections of avertine (1.25 g/

ml 2,2,2-tribromoethanol in 2.5% tert-amyl-alcohol; 20  $\mu$ l/g bodyweight). Animals were killed with overdose of intraperitoneal avertine (100  $\mu$ l/g bodyweight) after the eyes had been removed. All efforts were made to minimize animal discomfort and suffering.

Mice were rd10 mutants (B6.CXB1-Pde6brd10/J, on a C57Bl6J background) [13] and wild-type (C57BL/6J; WT), both from Jackson. The presence of the homozygous Pde6b mutation was assessed periodically with PCR on DNA extracted from tail tissue as explained previously [14]. The primers were: RD10-F: CTT TCT ATT CTC TGT CAG CAA AGC) and RD10-R: CAT GAG TAG GGT AAA CAT GGT CTG). The corresponding PCR amplification was performed in 30 cycles by denaturation at 94 °C for 3 min; annealing at 94, 60 and 72 °C, respectively, for 1 min, 30 s and 1 min. Elongation was at 72 °C for 7 min. The product obtained was purified and digested with HhaI enzyme (New England BioLabs, Ipswich, MA), whose restriction site is not included in the rd10 mutant DNA. After 2-hrs incubation at 37 °C, the digested DNA was run upon a 3% Metaphor Agarose (Lonza, Rockland, ME) for separation of short DNA fragments. The homozygous rd10 mutation is revealed by the presence of a single band of 97 base pairs.

**Enriched environment:** The enriched environment consisted of large (60  $\times$  38  $\times$  20 cm) Plexiglas cages containing a running wheel, two transparent Plexiglas tunnels, hard-pressed cardboard nesting material, and six to eight small, hard plastic objects that were replaced on a weekly basis. An rd10 female was placed in an enrichment cage with a male. When pregnancy started, five additional rd10 females, previously mothers (helpers), were added to the cage. The rd10 progeny (usually six to eight pups) remained in the same enriched environment up to P30; afterward, the males and females were separated and kept in enrichment cages until the final behavioral testing and/or retinal examination.

**Standard environment:** Control animals were rd10 mice born and raised in the same room, on the same 12 h:12 h light-dark cycle, with illumination levels below 100 lux (measured periodically with a lux meter placed inside the cages). All mice (EE and ST) were administered the same diet, with water and food ad libitum. Control cages were smaller standard laboratory cages (42  $\times$  26  $\times$  18 cm), without objects and hosting only the pregnant female and, later, her litter. After P30, the mice were separated from their mother, and only three to four individuals were hosted in each cage.

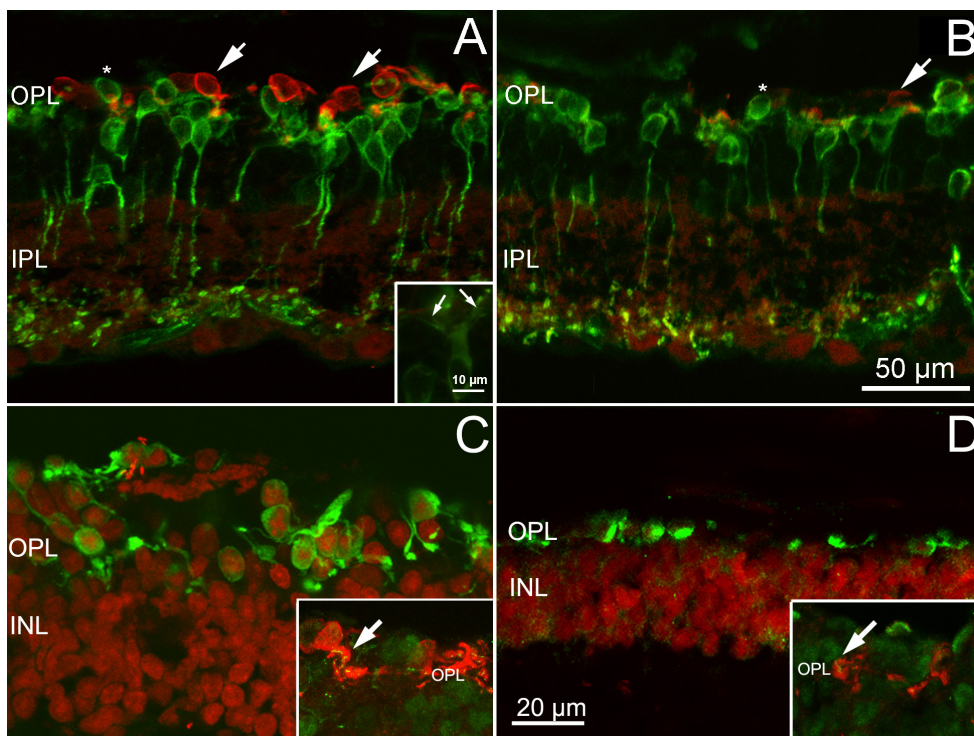


Figure 2. Cones and bipolar cells in EE and ST mice. Vertical retinal sections from rd10 EE (A) and rd10 ST (B) mice stained with M/L and S cone-opsin (red signal) and PKC alpha (green signal) antibodies. The number of residual cones is higher in the enriched environment (EE) samples (arrows). There are no major differences between the two groups of animals in the morphology of rod bipolar dendritic trees, which appear retracted almost completely in the two samples, with the exceptions of scattered dendrites emerging from the cell bodies of some rod bipolar cells in the EE retinas (arrows in inset). Some bipolar cell somas are misplaced in the outer retina, at the same height as the photoreceptors (asterisk). C, D: Staining with cone arrestin antibodies (red signal) in

the rd10 EE (C) and rd10 ST (D) sections. Note the more elaborate shape of cones visible in C. Insets: High magnification of the OPL in which the cones are stained red with arrestin and the synaptic ribbons (arrows) green with ribeye antibodies. INL = inner nuclear layer; IPL = inner plexiform layer; OPL = outer plexiform layer.



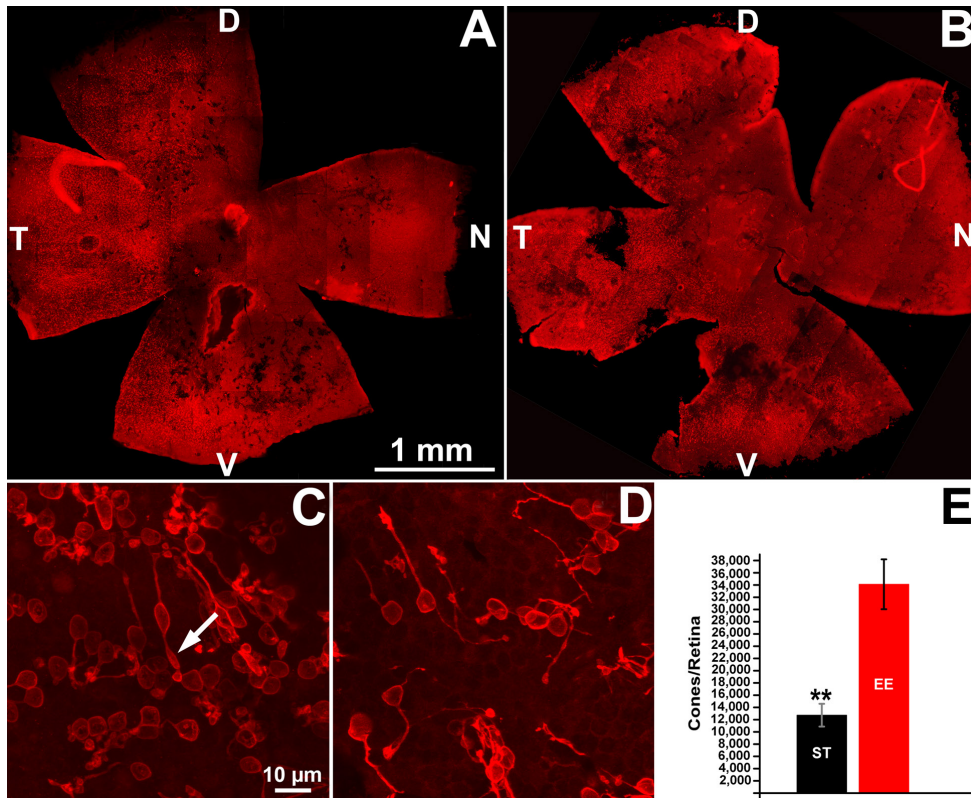


Figure 3. Cone survival in EE and ST mice. **A** and **B**: Retinal whole mounts from 1-year-old rd10 mice raised in EE (**A**) and ST conditions (**B**), stained with antibodies against cone-specific opsins (red signal). A large black area devoid of cones is evident in the central part of the retina, revealing a nasal-temporal pattern of degeneration. Cone clusters (visible as red, punctate areas) are still preserved in the periphery of both retinas. These low magnification images show retinal tears that form easily in the standard laboratory (ST) samples during dissection (**B**). **D**, **V**, **N**, **T**: dorsal, ventral, nasal, temporal retinal poles. **C** and **D**: High-magnification confocal images of cones obtained from the retinal samples shown in **A** and **B**, at corresponding locations. Local density of cones is visibly higher in the enriched environment

(EE) compared to the ST sample. Typical cone remodeling is evident in both cases, but the EE cones display apical protrusions reminiscent of residual outer segments (arrow). **E**: Counts from four retinas in each group show that the rd10 EE mice at 1 year have almost three times as many surviving cones ( $34,000 \pm 4,000$ ) as the ST control mice ( $12,700 \pm 1,800$ ) *t* test,  $**p=0.003$ .

**Retinal immunocytochemistry:** At the age of exactly 1 year, the rd10 mice kept in EE and ST conditions and the WT, the control mice, also kept in an ST environment, were deeply anaesthetized as described, their eyes quickly enucleated, and a reference point taken on the dorsal pole with a tissue ink marker. A total of eight rd10 mice (four EE and four ST) and four WT mice were used for immunocytochemistry (ICCH) on vertical retinal sections. Whole eyes were immersion-fixed in 4% paraformaldehyde (PAF) in 0.1 M phosphate buffer, rinsed, sucrose-infiltrated, embedded in optimal cutting temperature (OCT) medium, and serially sectioned at 12  $\mu$ m on a cryostat.

Immunostaining on vertical sections and confocal microscopy (Leica TCS-LP confocal microscopes, Leica, Milan, Italy) were performed as explained in [12]. Briefly, retinal sections were incubated overnight, at 4 °C, in primary antibodies, diluted in a solution of PBS (1X; 120 mM NaCl, 20 mM KCl, 10 mM NaPO<sub>4</sub>, 5 mM KPO<sub>4</sub>, pH 7.4), containing 0.1% Triton X -100 and 1% bovine serum albumine (BSA). The presence of rods was assessed by staining with rhodopsin (RET-P1, O4886) antibodies (Sigma-Aldrich, Milan, Italy;

used at 1:1,000 dilution); cone morphology and number were assessed by using antibodies against cone red/green (L/M) opsin (Millipore AB5404; from Applied Biosystems, Monza, Italy) and cone blue (S) opsin (Millipore AB5407), used at 1:1,000 dilution; cone-arrestin (Millipore AB15282; used at 1:5,000 dilution) antibodies were also used. The morphology of the rod bipolar cells, cone bipolar cells, and horizontal cells was studied using antibodies against protein kinase C-alpha (PKC alpha; Sigma, P5704; used at 1:1,000 dilution), synaptotagmin-2 (ZNP1, Zebrafish International Resource Center (Eugene, OR); used at 1:1,000 dilution), and calbindin-D-28K (Swant CB-38a, Marly, Switzerland; used at 1:1,000 dilution), respectively. Amacrine and ganglion cells were studied with antibodies against ChAt (AB114P; Chemicon, Applied Biosystems; used at 1:1,000 dilution), calretinin C7699/4 Swant; used at 1:1,000 dilution), and neurofilament (Sigma N0142; used at 1:200 dilution), respectively. Ribbon synapses were labeled with a ribeye antibody (CtBP2, BD Transduction, Milan, Italy; used at 1:500 dilution). A melanopsin antibody (UF006; used at 1:2,000 dilution) that recognizes a subset of ganglion cells was kindly donated by Ignacio Provencio (University of Virginia).

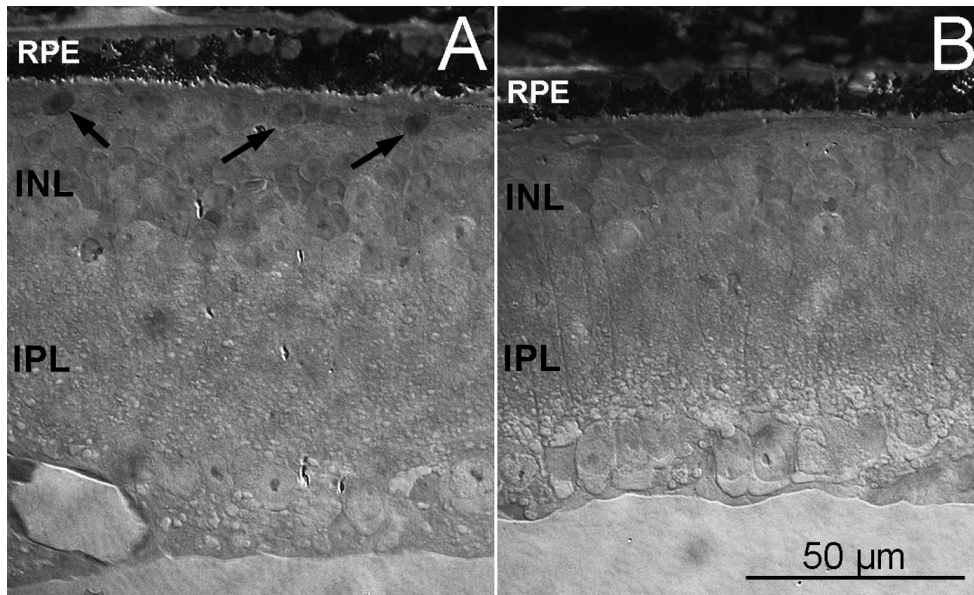


Figure 4. The outer retina in in EE and ST mice. Semithin (2  $\mu\text{m}$  thick) plastic sections from the retinas of rd10EE (A) and rd10 ST (B) mice, obtained at similar locations. The retina in A is thicker and shows a layer of scattered cell bodies (arrows) abutting the RPE. In A and B, sparse granules of RPE pigment (visible as bright, elongated drops) penetrate the neural retina. INL = inner nuclear layer; IPL = inner plexiform layer.

Secondary antibodies were anti-rabbit, anti-goat, and anti-mouse immunoglobulins conjugated with Alexa Fluor 488 (A21202, Applied Biosystems) or with Rhodamine Red-X (Ab 711–295–152; Jackson ImmunoResearch, Suffolk, GB). They were diluted 1:1,000 in a solution containing 0.1% Triton X-100 and 1% BSA, in PBS. The overall survival of the retinal cells was assessed on vertical sections stained with micromolar concentrations of Hoechst or ethidium nuclear dyes.

**Immunofluorescence: Cone counting:** Cone counting was performed on retinal whole mounts as explained in [12]. Briefly, eyes (contralateral to those used for ICCH on vertical sections,  $n=4$ , rd10 EE; and  $n=4$ , rd10 ST) were treated as above, embedded in OCT, and stored at  $-20^\circ\text{C}$ . For whole mount staining, the eye cup were defrosted, the retinas isolated and deprived of pigmented epithelium, and four incisures were cut to identify the main quadrants. The retinas were then washed in 0.1 M PBS ( $3 \times 10$  min) and left overnight in a blocking solution with 0.5% Triton X-100 and 5% bovine serum albumin (BSA) in PBS (pH 7.4) at  $4^\circ\text{C}$ . The retinas were then placed in a solution of rabbit anti-Red/Green Opsin and anti-Blue Opsin antibodies (3 days at  $4^\circ\text{C}$ , 1:800), washed extensively, and then incubated in Rhodamine Red-X secondary antibodies. All solutions contained 0.3% Triton X-100, 0.5% BSA in PBS. Retinas were mounted flat in Vectashield (Burlingame, CA; photoreceptor side up) and systematically imaged with a (Peltier-cooled) Zeiss AxioCam color camera, interfaced with a Zeiss AxioScope fluorescence microscope (Zeiss, Milan, Italy), using a 5X objective. Images were assembled into single montages of the whole retinal

surface using Adobe PhotoMerge software. Using differences in labeling brightness, displayed on the images as color gradients, the cone clusters and three concentric zones (central, medium, and peripheral) of variable sizes were identified. The cone densities were estimated separately by counting cones on high-resolution confocal images obtained in each zone.

Serial optical sections were obtained at 0.5  $\mu\text{m}$  intervals along the z plane to encompass the entire thickness of the labeled cones. The scanning areas were 16 fields/retina  $375 \times 375 \mu\text{m}^2$ . The fields were regularly spaced along the dorso-ventral and nasotemporal retinal meridians. Cone counts were performed on serial reconstructions obtained by stacking the focal series (usually four consecutive planes, each 0.5  $\mu\text{m}$  thick), with Metamorph software. Locally estimated cone densities were assigned to the corresponding zones of each retinal map. Total numbers of cells were obtained by multiplying the average cellular densities by the area of the corresponding retinal zone. Statistical analysis (*t* test) was performed with OriginPro 7.0.

**Electron microscopy:** Mice aged 1 year (rd10 EE,  $n=3$ ; rd10 ST,  $n=3$ ; WT,  $n=4$ ) were anesthetized, and their eyes quickly enucleated after taking a reference point on the dorsal pole with a tissue ink marker. Routine EM was performed as previously described [15]. Briefly, whole eyes were fixed for 30 min in 2% PAF, 2.5% glutaraldehyde in 0.1 M phosphate buffer (PB), pH 7.4. Then, they were cut at the ora serrata, the anterior segments removed, and the eye cups fixed for a total of 12 h at  $4^\circ\text{C}$ . Small triangular blocks were dissected maintaining reference points for retinal location and eccentricity;



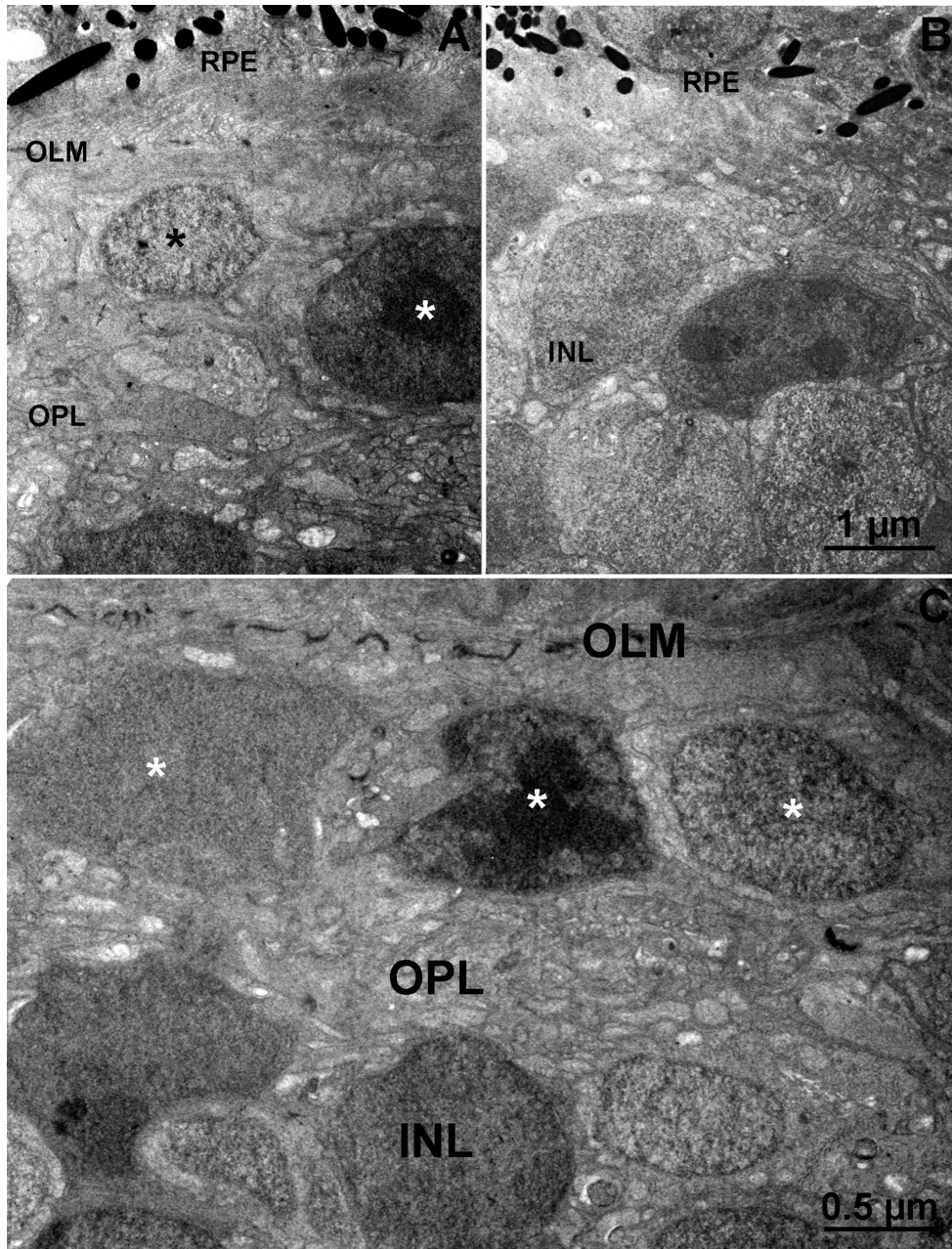


Figure 5. Ultrastructure of the outer retina in EE and ST mice. Electron micrographs of the outer retina of EE (A, C) and ST (B) rd10 mice. Asterisks in the enriched environment (EE) sample label nuclei of residual cells in the outer retina, adjacent to a well-organized outer limiting membrane (OLM). These nuclei have different densities and presumably belong to surviving cones and misplaced bipolar cells. The outer plexiform layer (OPL) is still present in A and C, while in the ST sample (D), the cell bodies of the inner nuclear layer (INL) cells are in close proximity to the RPE.

the sclera and choroid were detached, and the retina with the pigment epithelium was rinsed in PB for 1 h, postfixed in 2% osmium tetroxide for 2 h, bloc stained with 1% uranyl acetate, dehydrated in ethanol, and flat embedded in Embed 812/Araldite (Electron Microscopy Sciences, Hatfield, PA). Ultrathin sections were stained with uranyl acetate and lead citrate and examined with a Jeol 1200 EXII (Jeol, Milan, Italy) electron microscope. Images of the outer retina were obtained with a charge-coupled device (CCD) Olympus Veleta Megaview (Olympus, Münster, Germany) camera at

20,000X, transferred to an image analysis workstation, and examined offline.

*Behavioral test: Visual acuity:* Visual acuity was assessed at 365 days using the visual water task under photopic conditions using a water maze originally developed by Prusky [16]. The stimuli were computer-generated square-wave black-and-white gratings with a fixed luminance of 39.95 cd/m<sup>2</sup> with spatial frequencies ranging between 0.087 and 0.550 cycles/degree.



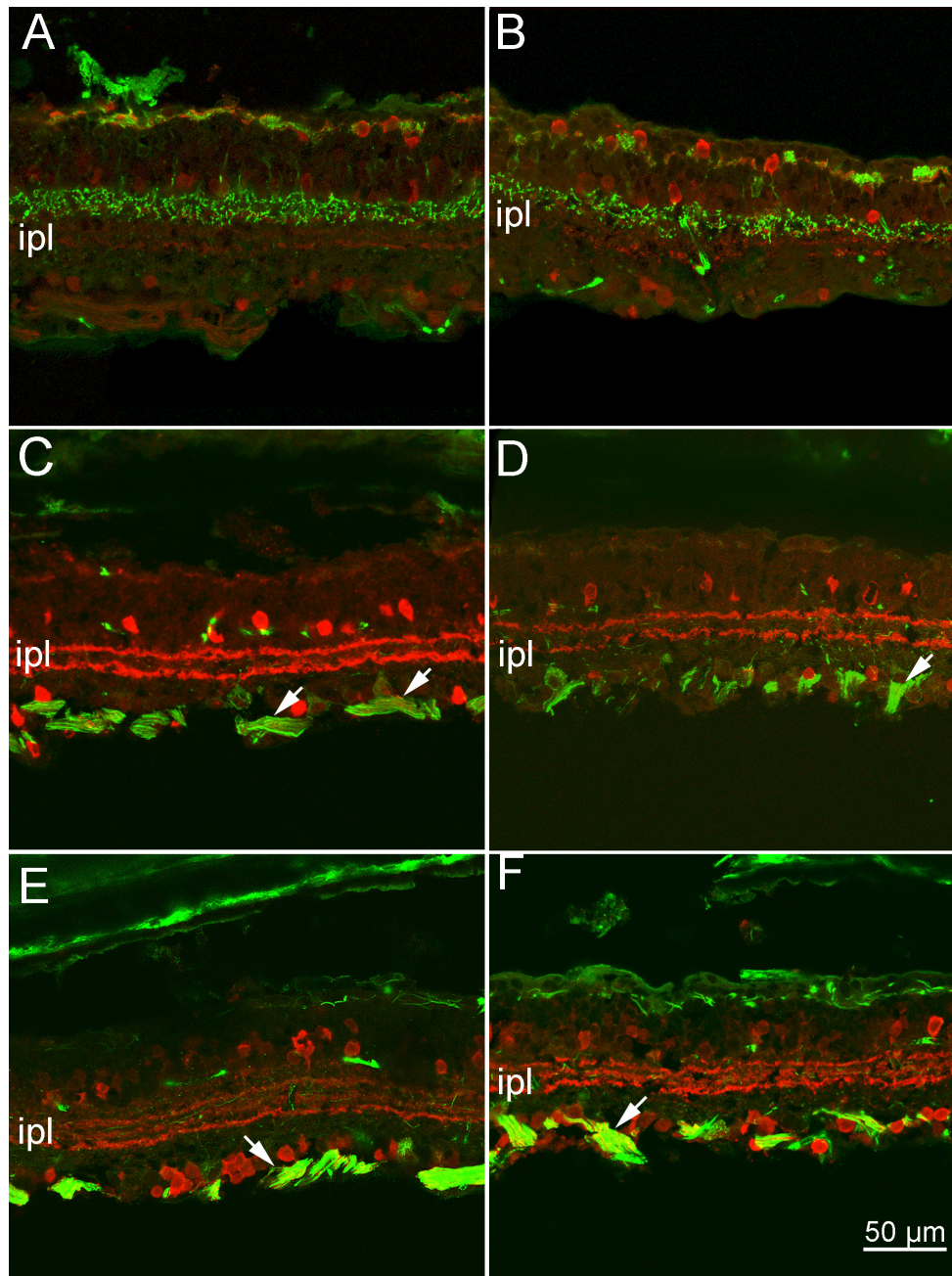


Figure 6. The inner retina of EE and ST mice. Antibody staining of retinal cell types in rd10 mice, kept in EE (A, C and E) and in ST conditions (B, D, and F), respectively. A and B: Znpl staining of cone bipolar cells (green signal) reveals extensive loss of dendrites in the outer plexiform layer (OPL) of the samples in A and B and better preservation of axonal arbors in the inner plexiform layer (IPL) of the enriched environment (EE) retinas (A). Horizontal cells (red signal) stained with calbindin D antibodies appear devoid of dendrites in both cases. C and D: Cholinergic amacrine cells, stained with ChAT antibodies (red signal), are well preserved in the EE (C) and standard laboratory (ST) (D) samples, and the two parallel, cholinergic bands run in the IPL at the expected heights. Similarly, ganglion cells, stained green by neurofilament antibodies, are well preserved, with axons running in bundles (arrows). E and F: Calretinin staining of amacrine cells (red signal) reveals the three dendritic bands regularly laminating the IPL, in the EE (E) and ST (F) retinas. Neurofilament labeling (green signal) shows fine ganglion cell dendrites running in the IPL and fiber clusters (arrows) at the inner retinal aspect. In the outer retina, residual processes belonging to axonal arborizations of horizontal cells are lightly stained in both specimens.

As described previously [12], the mice were initially trained at 30 days of age. Once they learned to associate the platform with the lowest frequency grating, the frequency was increased progressively until the mice could no longer locate the platform. The highest frequency recognized was recorded as a marker of visual acuity. Mice were regularly trained once a month until to the final test.

## RESULTS

In a previous work [12], we demonstrated that early exposure to an EE is a powerful tool for extending the time window of photoreceptor viability in rd10 mice, consistently preserving retinal structure and function beyond the period observed in these mutants when they are raised in standard laboratory conditions. In the present study, we used morphological and behavioral methods to demonstrate that, in the same mutant mouse, an EE can delay retinal decay in the long term,

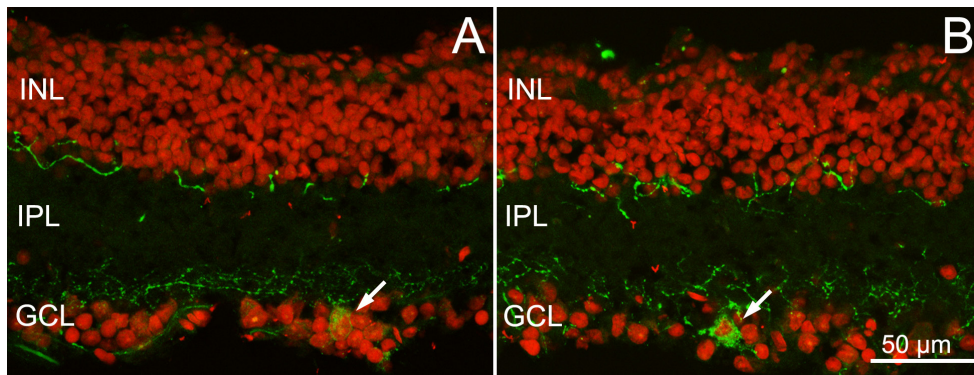


Figure 7. Melanopsin ganglion cells in EE and ST mice. Melanopsin staining (green signal) of retinal sections from EE (A) and ST (B) rd10 mice. Red: nuclear counterstaining. Note the two plexa formed by the dendrites of the melanopsin ganglion cells at different depths in the inner plexiform layer (IPL). Arrows point to cell bodies. INL = inner nuclear layer; GCL = ganglion cell layer.

maintaining a lasting population of cones and a residual vision in photopic conditions.

*Retinal morphology in EE and ST rd10 mice at 1 year of age:* Fluorescence nuclear staining of vertical sections from retinas of rd10 mice aged 1 year showed an expected and extensive loss of photoreceptors compared to the retinas of the WT, control mice. The outer nuclear and outer plexiform layers were almost undetectable in the mutants (Figure 1). Samples from the EE and ST rd10 animals appeared similarly degenerated, but the retinas from the EE mice were thicker and better preserved than those from the ST counterparts (Figure 1), which were also extremely fragile during the dissection and the histological procedure.

Antibody staining of the photoreceptors showed that virtually no rods were left in the experimental groups (not shown) while cone-opsin positive cells occurred frequently in the EE retinas compared to the ST retinas. These residual cones were mostly located in the retinal periphery and were arranged at the expected location, just below the outer limiting membrane, where they formed a single, discontinuous layer (Figure 2). Arrestin-antibody staining labeled the cells in their entirety and showed that in the retinas from the EE mice the residual cones showed a clear polarity, with elongated processes terminating in small, round endings (Figure 2C,D). Punctate ribbons could be labeled with ribeye antibodies. Conversely, in the retinas from ST mice, the cones were ovoid, with rare endings and few ribbons (Figure 2C,D).

Fluorescence microscopy of the whole mount retinas stained with cone-specific opsins was used for topographical counting of the cones in the EE and ST mice. Low-magnification images confirmed that cones were more abundant in the peripheral retina and occurred in clusters, separated by large areas totally devoid of labeled profile (Figure 3A,B). A nasal-to-temporal pattern of degeneration was visible. Remodeling was evident in the retinas from the EE and ST mice, insofar residual cones had enlarged, ovoid bodies, often

with the major axis oriented parallel to the outer limiting membrane (Figure 2A) and thin, long telodendria running a tangential course in the remnant outer plexiform layer (OPL; Figure 3C,D). These residual cones were similar to those described in analogous models of RP [17]. However, whole mount staining confirmed that the cones from the EE mice retained a morphology more reminiscent of their original shape, with a better defined polarity and, occasionally, a fragment of an outer segment (Figure 3C). Cell counting showed that the 1-year-old rd10 EE mice had almost three times as many surviving cones ( $34,000 \pm 4,000$ ) as the ST control mice ( $12,700 \pm 1,800$ ; *t* test,  $p=0.003$ ; Figure 3).

Analysis of the vertical semithin sections consistently confirmed the presence of a single, discontinuous layer of elongated cells in the outer retinas of the EE mice but not in the ST mice (Figure 4). Electron microscopy showed that

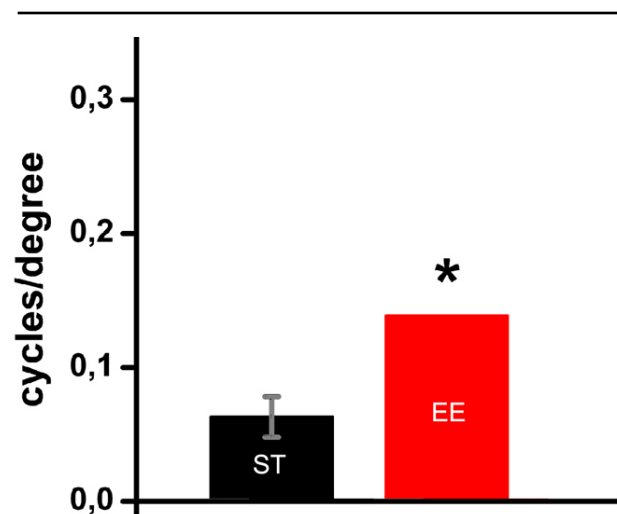


Figure 8. Visual behavior. Visual acuity of 1-year-old rd10 mice is significantly higher in EE than in the age-matched ST tested mice. Student *t* test,  $*p=0.029$ . Each column shows the mean (and standard error of the mean, SEM) of four animals for each groups. The error bar for the enriched environment (EE) group is undetectable.



these cells were positioned in the outermost retinal tier, abutting a clearly identifiable outer limiting membrane (Figure 5), and were largely occupied by a nucleus with a variable ultrastructure: Some nuclei had highly condensed chromatin (similar to that of normal rods), while others were more homogeneous (Figure 5A,D). Most likely, they included the residual population of cones, as well as the cell bodies of some bipolar cells, which are known to move toward the outer retina when photoreceptors die out [18], as shown in Figure 2 (asterisks). No outer segments were evident in individual EM sections. The outer plexiform layer, instead, although thinned, was clearly visible and occupied by processes with an irregular course (Figure 5A,D). The examination of sections from retinal samples with matching eccentricity and location showed that rare small cells persisted in the outer retinas of the rd10 mice kept in ST conditions. The OPL was not recognizable, and the cells of the inner nuclear layer (INL) were adjacent to the retinal pigment epithelium (Figure 5B).

The use of cell type-specific antibodies showed that, at 1 year of age, the inner retinas of the EE and ST mice of the rd10 strain were similarly remodeled. Rod bipolar cells stained with PKC alpha antibodies confirmed the previously described impoverishment of their dendritic arborizations (Figure 2). The cell bodies, devoid of outward-directed dendrites, were elliptical and at times were misplaced in the outer nuclear layer, intermingled with the somas of residual cones (Figure 2). In the retinas from the EE mice, residual dendrites (and occasional sprouts) were more often observed (Figure 2A, inset). Znp-1 (synaptotagmin) staining of subsets of cone bipolar cells showed better preservation of axonal arbors in the inner plexiform layer (IPL) of the EE mice than of the ST rd10 mice, while calbindin D staining of the horizontal cells showed major withdrawing of processes in the OPL of both preparations (Figure 6A,B). Cholinergic amacrine cells and, more generally, the laminar organization of the amacrine cell processes in the IPL were equally well maintained in both experimental groups, as shown by the ChAt and calretinin antibodies (Figure 6C–E). Finally, ganglion cells, stained with neurofilament antibodies, were well preserved in both experimental groups (Figure 6C–F). Their cell bodies, dendrites, and axons in the optic nerve layer were clearly visible, with no apparent abnormalities. A population of melanopsin-positive ganglion cells was clearly detectable after staining with a selective antibody (Figure 7). Their dendrites made two plexa at different depths in the IPL: a thin one, adjacent to the amacrine cell bodies, and a thicker one, adjacent to the ganglion cell layer. The dendrites of these cells were profusely ramified and well preserved in the retinas of the EE and ST mice.

In summary, antibody staining at 1 year of age showed the expected, regressive remodeling of second-order neurons in the retinas of rd10 mice in the EE and ST experimental groups, and proportionally better preservation of the deepest part of the inner retina (i.e., constituted by amacrine and ganglion cells), in addition to the population of persisting cones in the EE samples.

*Visual behavior:* Behavioral tests aimed at assessing visual acuity in photopic conditions demonstrated that, at 1 year of age, the rd10 EE mice were still capable of performing the visual water task, with a residual acuity of 0.14 c/dg in the photopic range, unlike the ST age-matched rd10 mice (0.06 c/dg; Figure 8).

## DISCUSSION

It is well-known that in RP photoreceptors are doomed to death and blindness is the inevitable outcome. However, since the natural course of the disease is usually slow, any successful attempt to delay progression further can itself be considered a cure.

In our recent work [12], we reported that rd10 mice, a well-established model of autosomal recessive RP caused by a rod-specific mutation, when raised from birth in enriched conditions undergo a slower process of retinal degeneration and exhibit correspondingly better-preserved retinal morphology, photoreceptor capability to respond to light stimuli, and retention of visual acuity and contrast sensitivity over time. The effects of an EE are associated with concomitant increases in retinal levels of ciliary neurotrophic factor (CNTF), a molecule with the documented capability to delay photoreceptor degeneration in various animal models and tested in clinical trials on humans [19], and of mammalian target of rapamycin (mTOR), a fine sensor of cell and tissue metabolism. Here, we investigated the long-term effects of an EE on the same rd10 mutants born and maintained in such an environment up to 1 year of age.

With morphological and quantitative analysis, we demonstrated an EE had a clear effect upon cone survival, insofar as almost three times as many cones persisted in the retinas of the EE rd10 mice compared to the ST controls. We failed to record an electroretinogram (ERG) from the retinas of the 1-year-old EE and ST mice. However, this can be explained by the fact that, even in the retinas of the EE mice, the absolute number of surviving cones was low, and their spatial arrangement sparse. Collectively, the light response they generated was probably too small to produce a measurable ERG. Similarly, in patients with low vision only recordings of local ERG responses with focal techniques can unmask retinal areas with residual light sensitivity [20]. Indeed, in the

rd10 EE retinas studied here, the cones retained immunoreactivity for cone-specific opsins and cone arrestin, indicating that proteins specifically involved in phototransduction initiation and deactivation were preserved, even in the absence of visible outer segments. Moreover, the cones also maintained synaptic ribbons, pointing out the persistency of connections in the residual OPL. Indeed, visual acuity, which is set in the first place by cone density and which we measured with the Prusky visual task, although low, was higher in the EE mice, indicating the maintenance of some form of cone-mediated vision. We deliberately chose this method of visual performance since it provides information on the integrity of the entire visual pathway and the behavioral relevance of the therapeutic protocol adopted here.

Morphologically, the inner retinas of the EE rd10 mice were only slightly better preserved (thicker and less fragile) than those of the ST counterparts. In the end, the major distinction between the two experimental groups was the higher density of cones and the preserved visual acuity. We conclude that prolonged enrichment slows down retinal degeneration in the long term, protecting retinal cones. However, since the number of these photoreceptors in a wild-type mouse of the C57Bl6 strain is around 180,000 [21], it is evident that the EE and ST mice underwent major cone loss as a secondary effect of the primary rd10 mutation.

It cannot be excluded that the preservation of visual responses behaviorally detected in the EE mice is partly due to a direct effect of the EE on the melanopsin ganglion cells, previously shown and confirmed here to survive in retinal degeneration mice [22]. Upon exposure to an enriched environment, melanopsin ganglion cells could plastically enhance their efficiency in transmitting ambient light intensity information to the imaging-forming visual system [23], contributing to the preservation of visual abilities. In addition, enhancement or maintained activation of overall visual cortical plasticity, demonstrated in other aging rodents exposed to an EE [24], could participate in the residual visual functions of the EE mice. More dedicated studies, also based on recordings of visually evoked potentials, are needed to address this issue specifically.

The molecular determinants mediating the effects of an EE are poorly understood, but it is now clear that environmental factors affect the expression of molecules that regulate cellular metabolism. For instance, CNTF, a neurocytokine increased in the EE conditions, reduces the inflammatory signaling cascades associated with lipid accumulation by centrally regulating the mechanisms of food intake [25]. In turn, decreased inflammation can contribute to ameliorating the reaction to injury and/or to pathological

conditions. Similarly, an enriched environment increases brain-derived neurotrophic factor (BDNF), which, in turn, exerts sympathoneural modulation of fat metabolism, overall leading to improved metabolic condition and cognitive state [26]. Indeed, aerobic exercise per se protects photoreceptors from light-induced damage through the BDNF-TrkB signaling pathway [27]. Remarkably, it has been suggested that the molecular determinants and mechanisms implicated in neuronal plasticity and typically associated with youth are maintained throughout life and support neuronal survival and repair during aging as well.

From a therapeutic standpoint, the demonstration that the beneficial effects of such a complex environmental manipulation upon retinal cones are long lasting when the stimulating environment is maintained is encouraging. The data shown here reinforce the notion that, like other parts of the brain, the retina is sensitive to manipulations capable of promoting CNS plasticity and repair in general. Indeed, these data expand to a pathological condition the recently provided demonstration that the retina is highly responsive to an EE during early and late development [28-31], with effects mediated by neurotrophic factors, long known to exert a protective action on the pathological conditions of this organ [32]. In addition to our studies on RP models, recent data show that an EE is capable of protecting the rodent retina against glutamate-induced toxicity [33] and ischemic damage [34], thus widening the range of pathological paradigms that obtain beneficial effects from this experimental manipulation. The results reported here should encourage the exploration of application of an EE, alone or in combination with other approaches, as a strategy for delaying vision loss in patients with RP awaiting a decisive remedy.

## ACKNOWLEDGMENTS

These studies were funded by the Velux STIFTUNG Foundation, CH (Prog. 691 to ES) and by the Italian CNR. The Authors are indebted to Drs. Maria Cristina Cenni and Alessandro Sale for critically reading the manuscript.

## BIBLIOGRAPHY

1. Kolesnikov AV, Fan J, Crouch RK, Kefalov VJ. Age-related deterioration of rod vision in mice. *J Neurosci* 2010; 30:11222-31. [PMID: 20720130].
2. Lehmann K, Schmidt KF, Lowel S. Vision and visual plasticity in ageing mice. *Restor Neurol Neurosci* 2012; 30:161-78. [PMID: 22348872].
3. Baroncelli L, Sale A, Viegi A, Maya Vetencourt JF, De Pasquale R, Baldini S, Maffei L. Experience-dependent



- reactivation of ocular dominance plasticity in the adult visual cortex. *Exp Neurol* 2010; 226:100-9. [PMID: 20713044].
4. Nithianantharajah J, Hannan AJ. Enriched environments, experience-dependent plasticity and disorders of the nervous system. *Nat Rev Neurosci* 2006; 7:697-709. [PMID: 16924259].
  5. Sale A, Berardi N, Maffei L. Environment and brain plasticity: towards an endogenous pharmacotherapy. *Physiol Rev* 2014; 94:189-234. [PMID: 24382886].
  6. Sale A, Maya Vetencourt JF, Medini P, Cenni MC, Baroncelli L, De Pasquale R, Maffei L. Environmental enrichment in adulthood promotes amblyopia recovery through a reduction of intracortical inhibition. *Nat Neurosci* 2007; 10:679-81. [PMID: 17468749].
  7. Shintani K, Shechtman DL, Gurwood AS. Review and update: current treatment trends for patients with retinitis pigmentosa. *Optometry* 2009; 80:384-401. [PMID: 19545852].
  8. Daiger SP, Sullivan LS, Bowne SJ. Genes and mutations causing retinitis pigmentosa. *Clin Genet* 2013; 84:132-41. [PMID: 23701314].
  9. Sahni JN, Angi M, Irigoyen C, Semeraro F, Romano MR, Parmeggiani F. Therapeutic challenges to retinitis pigmentosa: from neuroprotection to gene therapy. *Curr Genomics* 2011; 12:276-84. [PMID: 22131873].
  10. Yang Y, Mohand-Said S, Danan A, Simonutti M, Fontaine V, Clerin E, Picaud S, Léveillard T, Sahel JA. Functional cone rescue by RdCVF protein in a dominant model of retinitis pigmentosa. *Mol Ther* 2009; 17:787-95. [PMID: 19277021].
  11. Gargini C, Terzibasi E, Mazzoni F, Strettoi E. Retinal organization in the retinal degeneration 10 (rd10) mutant mouse: a morphological and ERG study. *J Comp Neurol* 2007; 500:222-38. [PMID: 17111372].
  12. Barone I, Novelli E, Piano I, Gargini C, Strettoi E. Environmental enrichment extends photoreceptor survival and visual function in a mouse model of retinitis pigmentosa. *PLoS ONE* 2012; 7:e50726-[PMID: 23209820].
  13. Chang B, Hawes NL, Hurd RE, Davisson MT, Nusinowitz S, Heckenlively JR. Retinal degeneration mutants in the mouse. *Vision Res* 2002; 42:517-25. [PMID: 11853768].
  14. Mazzoni F, Novelli E, Strettoi E. Retinal ganglion cells survive and maintain normal dendritic morphology in a mouse model of inherited photoreceptor degeneration. *J Neurosci* 2008; 28:14282-92. [PMID: 19109509].
  15. Strettoi E, Mears AJ, Swaroop A. Recruitment of the rod pathway by cones in the absence of rods. *J Neurosci* 2004; 24:7576-82. [PMID: 15329405].
  16. Prusky GT, West PW, Douglas RM. Behavioral assessment of visual acuity in mice and rats. *Vision Res* 2000; 40:2201-9. [PMID: 10878281].
  17. Lin B, Masland RH, Strettoi E. Remodeling of cone photoreceptor cells after rod degeneration in rd mice. *Exp Eye Res* 2009; 88:589-99. [PMID: 19087876].
  18. Strettoi E, Pignatelli V. Modifications of retinal neurons in a mouse model of retinitis pigmentosa. *Proc Natl Acad Sci USA* 2000; 97:11020-5. [PMID: 10995468].
  19. MacDonald IM, Sauve Y, Sieving PA. Preventing blindness in retinal disease: ciliary neurotrophic factor intraocular implants. *Can J Ophthalmol* 2007; 42:399-402. [PMID: 17508034].
  20. Hood DC, Holopigian K, Greenstein V, Seiple W, Li J, Sutter EE, Carr RE. Assessment of local retinal function in patients with retinitis pigmentosa using the multi-focal ERG technique. *Vision Res* 1998; 38:163-79. [PMID: 9474387].
  21. Jeon CJ, Strettoi E, Masland RH. The major cell populations of the mouse retina. *J Neurosci* 1998; 18:8936-46. [PMID: 9786999].
  22. Semo M, Peirson S, Lupi D, Lucas RJ, Jeffery G, Foster RG. Melanopsin retinal ganglion cells and the maintenance of circadian and pupillary responses to light in aged rodless/coneless (rd/rd cl) mice. *Eur J Neurosci* 2003; 17:1793-801. [PMID: 12752778].
  23. Benarroch EE. The melanopsin system: Phototransduction, projections, functions, and clinical implications. *Neurology* 2011; 76:1422-7. [PMID: 21502603].
  24. Scali M, Baroncelli L, Cenni MC, Sale A, Maffei L. A rich environmental experience reactivates visual cortex plasticity in aged rats. *Exp Gerontol* 2012; 47:337-41. [PMID: 22329907].
  25. Matthews VB, Febbraio MA. CNTF: a target therapeutic for obesity-related metabolic disease? *J Mol Med* 2008; 86:353-61. [PMID: 18210031].
  26. Cao L, Choi EY, Liu X, Martin A, Wang C, Xu X, Durning MJ. White to brown fat phenotypic switch induced by genetic and environmental activation of a hypothalamic-adipocyte axis. *Cell Metab* 2011; 14:324-38. [PMID: 21907139].
  27. Lawson EC, Han MK, Sellers JT, Chrenek MA, Hanif A, Gogniat MA, Boatright JH, Pardue MT. Aerobic exercise protects retinal function and structure from light-induced retinal degeneration. *J Neurosci* 2014; 34:2406-12. [PMID: 24523530].
  28. Landi S, Cenni MC, Maffei L, Berardi N. Environmental enrichment effects on development of retinal ganglion cell dendritic stratification require retinal BDNF. *PLoS ONE* 2007; 2:e346-[PMID: 17406670].
  29. Landi S, Ciucci F, Maffei L, Berardi N, Cenni MC. Setting the pace for retinal development: environmental enrichment acts through insulin-like growth factor 1 and brain-derived neurotrophic factor. *J Neurosci* 2009; 29:10809-19. [PMID: 19726638].
  30. Landi S, Sale A, Berardi N, Viegi A, Maffei L, Cenni MC. Retinal functional development is sensitive to environmental enrichment: a role for BDNF. *FASEB J* 2007; 21:130-9. [PMID: 17135370].
  31. Sale A, Cenni MC, Ciucci F, Putignano E, Chierzi S, Maffei L. Maternal enrichment during pregnancy accelerates retinal

- development of the fetus. *PLoS ONE* 2007; 2:e1160-[PMID: 18000533].
32. LaVail MM, Unoki K, Yasumura D, Matthes MT, Yancopoulos GD, Steinberg RH. Multiple growth factors, cytokines, and neurotrophins rescue photoreceptors from the damaging effects of constant light. *Proc Natl Acad Sci USA* 1992; 89:11249-53. [PMID: 1454803].
  33. Szabadfi K, Atlasz T, Horváth G, Kiss P, Hamza L, Farkas J, Tamás A, Lubics A, Gábríel R, Reglodi D. Early postnatal enriched environment decreases retinal degeneration induced by monosodium glutamate treatment in rats. *Brain Res* 2009; 1259:107-12. [PMID: 19171125].
  34. Dorfman D, Fernandez DC, Chianelli M, Miranda M, Aranda ML, Rosenstein RE. Post-ischemic environmental enrichment protects the retina from ischemic damage in adult rats. *Exp Neurol* 2013; 240:146-56. [PMID: 23195592].

Articles are provided courtesy of Emory University and the Zhongshan Ophthalmic Center, Sun Yat-sen University, P.R. China. The print version of this article was created on 5 November 2014. This reflects all typographical corrections and errata to the article through that date. Details of any changes may be found in the online version of the article.